UCLA ENG-8734
Sept. 1987

THERMOMECHANICAL FORCE APPLICATION

Final Report for Summer 1987

(Sept. 30, 1987)

by

T. H. K. Frederking, P.I.
P. Abbassi
F. Afifi
W. E. W. Chen
P. K. Khandhar
D. Y. Ono

PREPARED FOR NATIONAL AERONAUTICS AND SPACE ADMINISTRATION

AMES RESEARCH CENTER, MOFFETT FIELD

CA 94035

Grant NAG2-464

UTILIZATION ON FEP ENERGETICS

Department of Chemical Engineering
School of Engineering and Applied Science
University of California, Los Angeles, CA 90024

UCLA ENG-8734
September 1987

THERMOMECHANICAL FORCE APPLICATION

Final Report for Summer 1987

(September 30, 1987)

by

T. H. K. Frederking, Principal Investigator
P. Abbassi
F. Afifi
W. E. W. Chen
P. K. Khandhar
D. Y. Ono

WITH SUPPLEMENT BY S. CASPI ET AL.

PREPARED FOR AERONAUTICS AND SPACE ADMINISTRATION
AMES RESEARCH CENTER, MOFFETT FIELD
CALIFORNIA 94035

Grant NAG2-464
UTILIZATION ON FEP ENERGETICS

Department of Chemical Engineering
School of Engineering and Applied Science
University of California, Los Angeles CA 90024

TABLE OF CONTENTS

1. ABSTRACT

The present work conducted in Summer 1987 continues investigations on "Thermal Components for 1.8 K Space Cryogenics" (Grant NAG 1-412 of 1986). The topics addressed are plug characterization efforts in a small pore size regime of sintered metal plugs, characterization in the non-linear regime, temperature profiles in a heat supply unit for a fountain effect pump and modeling efforts.

2. INTRODUCTION

The general task of fluid management in space has included the special challenge of moving and confining liquid Helium. This cryo-liquid has a very low surface tension. Therefore, some conventional confinement schemes for high surface tension liquids have not been employed on a large scale. Fortunately the quantum liquid He II, i.e. Helium-4 in its superfluid phase below 2.17 K, permits the utilization of thermomechanical forces (TM forces). Related developments of equipment for space application have been very encouraging. A first application area has been vapor-liquid phase separation (VLPS) using porous plugs. The TM force is directed into the tank interior to establish liquid confinement while permitting stable vapor venting. The "IRAS" observatory, a free flyer for far infrared night-sky observations, has been the initial successful system in this area.

Another application area is the fountain effect pump (FEP or thermomechanical pump). The TM force is directed in the desired pumping direction. In contrast to VLPS, the liquid mass flow rate desired is not in a simple co-current setup with respect to heat flow. The switch from VLPS to FEP operation has brought about an interest in smaller pore sizes than in VLPS work. The reason for the switch has been a low maximum fountain pressure difference in a single-stage device. As the pore size is decreased, the critical velocity is increased. Along with it the static pressure difference ΔP_T of the He II thermomechanics is raised. The permeability range is on the order of 10^{-11} cm^2, or even 10^{-12} cm^2. Smaller pore sizes are not of great interest at present because of a significant lambda point depression and a large space required for a specified liquid flow rate. The Darcy permeability (κ) is employed as a unique throughput measure. The related characteristic length $L_c = \kappa^{1/2}$ has been found to be a useful reference length in phenomenological equations.

An additional application area is the general utilization of the TM force in heat pumping/refrigeration systems. The latter in principle have the potential of contributing to a better energetics of an entire space flight duration as far as the He II bath functioning is concerned. In the general application area, several crucial components have been recognized as important devices. Examples are the pump core (porous plug), and related plugs for mechano-calorics, the heat exchanger system (thermal energy transfer system), the fluid acquisition device, possible venting components, e.g. VLPS, and connecting plumbing along with safety devices and instruments.

In the preceding period of Summer 1986, the FEP energetic effectiveness ("efficiency") has been a topic of interest using the transfer pump of our lab as example (Appendix A). The performance of the FEP in terms of the mass throughput versus the externally applied temperature difference ΔT has been studied. This work has resulted in "pump constants" evaluated by Dr. Yuan for various plugs. Prior to this work the mass transfer (volumetric transfer) effectiveness has been a subject of interest as the losses ought to be small for efficient fluid management. It turned out that this transfer "efficiency" has been quite close to 98% in the best cases. Thus little concern appeared to relate to this quantity. From the above loose use of "efficiency" ("effectiveness") terms, it is clear that a careful distinction of various definitions is necessary in order to avoid confusing interpretation. The energetics may not be as impressive as for a mechanical pump. The latter however is subject to cavitation danger in unprotected simple space operation. Therefore special measures have been tried to make the mechanical system "space flight ready".

For the FEP energetics the temperature difference ΔT plays a significant role since the second law of thermodynamics is not invalidated in the superfluid area. There are some peculiar constraints which modify the usual heat exchange conditions. Thus, the present work has continued thermal investigations of 1986 with the goal of understanding the optimum utiliza-

tion of TM force use better. In any case it is noted that there are always two extreme cases which may be inspected readily: one case is the very small temperature difference $\Delta T \ll T$. It results in a very small FEP energetic effectiveness. The other case is the large temperature difference, i.e. a cold side significantly below the lambda temperature ($T_\lambda = 2.17$ K). In that case the steep entropy-T function leads to the neglect of low-T terms and a simple result may be obtained. The energetic effectiveness, for instance is high at large ΔT and VLPS use for heat injection is characterized by very small volumetric losses. VLPS in space is easily accomplished as the vacuum of the environment is readily available without vacuum pump requirements of terrestrial magnet cooling systems.

The present report considers the progress made since activation of the present Grant NAG 2-464 in July 1987. The topics are treated as listed in the Table of Contents. Additional information is contained in Appendix sections. There have been additional experiments aiming at a more complete picture of porous media behavior. The data obtained are outlined as available at this time of report writing (September 1987).

3. PLUG CHARACTERIZATION: LINEAR REGIME ZNMF

ZNMF stands for Zero Net Mass Flow. This mode has been selected for the additional studies because of a "pump constant"/"plug constant" controversy. In some experiments with porous media, authors have seen similar "mutual friction" results for both, ZNMF modes and pump modes of FEP operation. The present work however, starting with the VLPS work and porous plug studies of S. W. K. Yuan and William A. Hepler, has revealed significant differences between FEP unit and VLPS system behavior. A clarification concerning ZNMF ought to cover a comparable range of porous plugs from the point of view of VLPS data. It turns out that the ZNMF range has been rather restricted at high ΔT. Therefore, several experimental runs have been conducted in the ZNMF mode. First, the linear range has been considered to obtain permeability results $\kappa(T)$ from the low-T analog of Darcy's law. Second, the non-linear range has been covered in order to obtain the rate constants of the turbulent regime.

The low-T permeability is accessible in a simple manner using the analog of Darcy's law for the He II thermomechanics. The usual pressure difference ΔP is replaced by the thermomechanical pressure difference ΔP_T. The latter is produced by an externally applied temperature difference ΔT. The temperature drives heat through the porous plug. Thus, instead of a mass flow of Darcy convection, the heat flow is of concern. The two-fluid model is used for quantification. According to this model, the heat flow is associated with flow of the normal fluid. The impeding property is the shear viscosity of the normal fluid. Therefore all quantities are quite similar to those of Darcy's law. The (superficial) normal fluid flow speed V_{no} is proportional to the Darcy permeability (κ), proportional to the pressure gradient $\left|\nabla P_T\right|$, and inversely proportional to the shear viscosity η_n. Thus

$$\kappa = V_{no}\eta_n / \left|\nabla P_T\right| \tag{3.1}$$

Figure 3.1 presents first an overview of carbon thermometer response for a particular plug of stainless steel with a permeability on the order of 10^{-10} cm^2. There are three different thermograms with T (in arbitrary units) as a function of time (t). The setup is sketched as inset in Figure 3.2.

The three thermograms (Fig. 3.1) show a low power input ($\dot{Q}$), an intermediate input and a high power input. For the linear regime discussion the low input is of interest. For details of similar thermograms the Ph.D. thesis of Dr. C. Chuang (UCLA 1981) and related publications may be consulted. Only small $\dot{Q}$-values permit the evaluation of the permeability.

The linear regime is accessible readily when there is laminar flow of the ZNMF mode. Figure 3.2 indicates this range. Most of the results though are in the non-linear range. The permeability is obtained readily from the linear domain response. From the thermograms the final result in ΔT has been deduced for infinitely long times. The ΔT is quite small for the present plug during laminar flow. Therefore a simplified calibration procedure is useful permitting fast data reduction: the resistance R of the thermometer as a function of the vapor pressure P_v is a monotonically decreasing function $R(P_v)$. To first order, this function is linear in log-log coordinates. The "slope" of the function is determined, and ΔT is deduced readily for small $\Delta T \ll T$. For this constraint the difference ΔT is about $\Delta R(dT/dR)$. Details of this calibration procedure for small temperature differences are given in Appendix D.

The permeability obtained is displayed in Figure 3.3 as a function of the bath temperature.

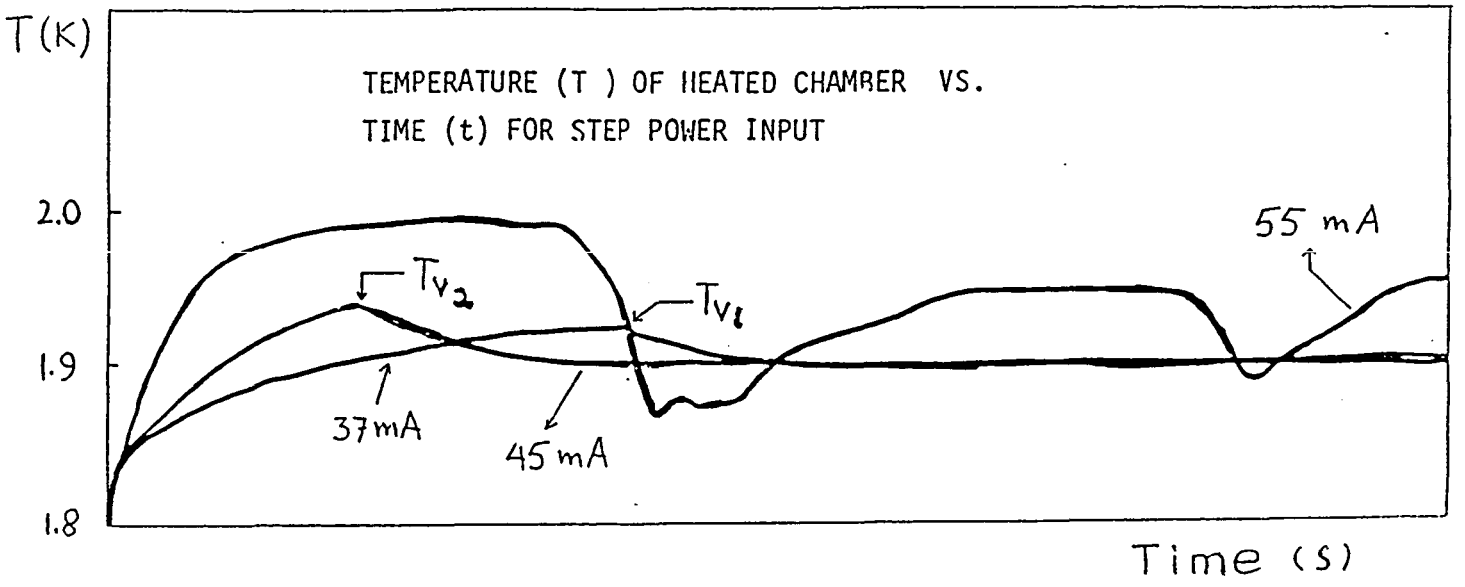

Figure 3.1. Thermograms of step inputs in heater power Q : Temperature versus time for various heater currents of plug K 10 S 02 - 6.4 x 0.75

Low power run: T increases with t until drop occurs at T_{V1}

Intermediate Q : T increases up to T_{V_2} The time at $T_{V}2$ is shorter than at T_{V1}.

High Q: Non-linear T-oscillations are observed

Note: The permeability is available at low power when the time reaches infinity.

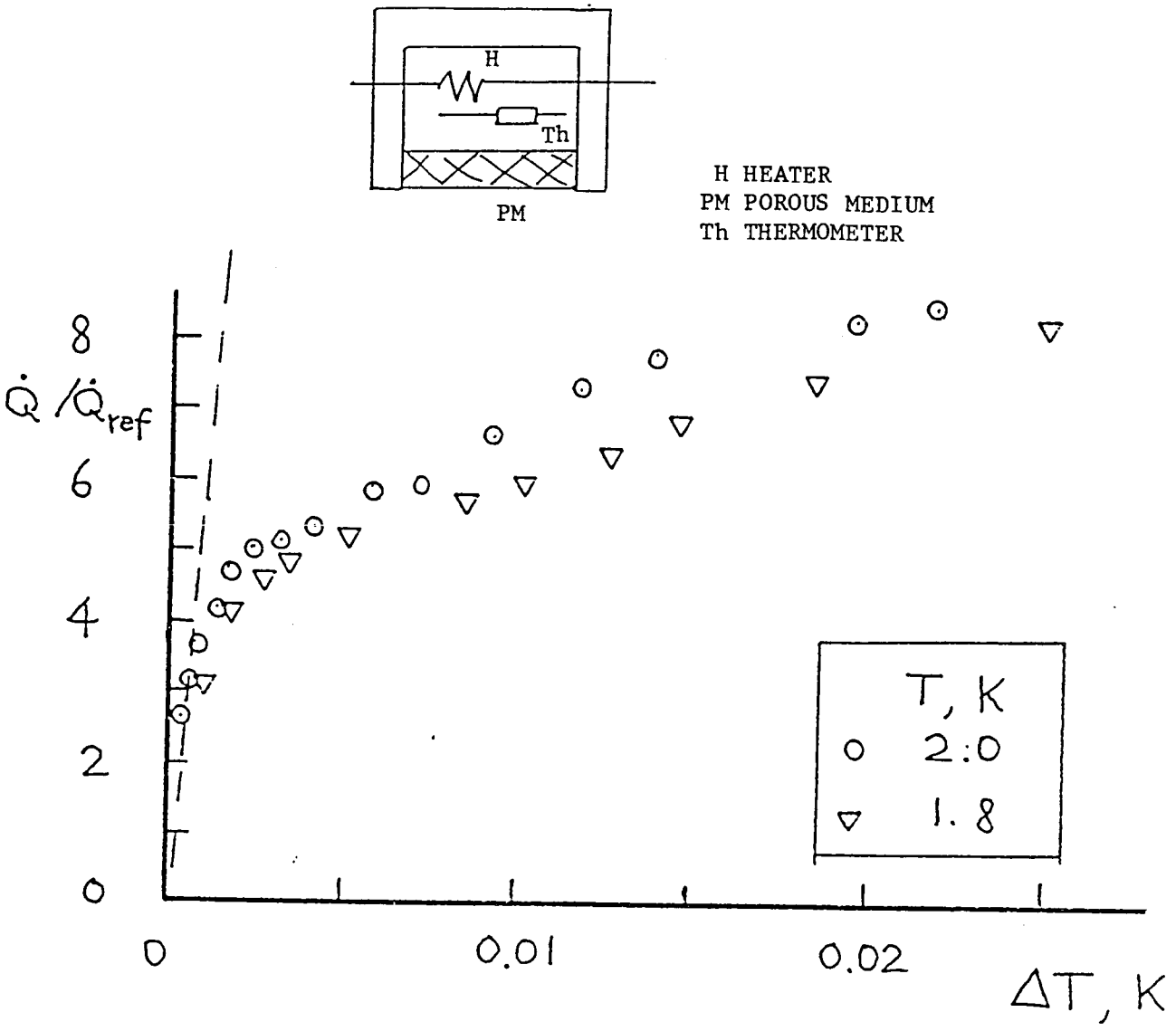

Figure 3.2. Heater power presented in normalized form as $\dot{Q}/\dot{Q}_{ref}$ vs. ΔT.

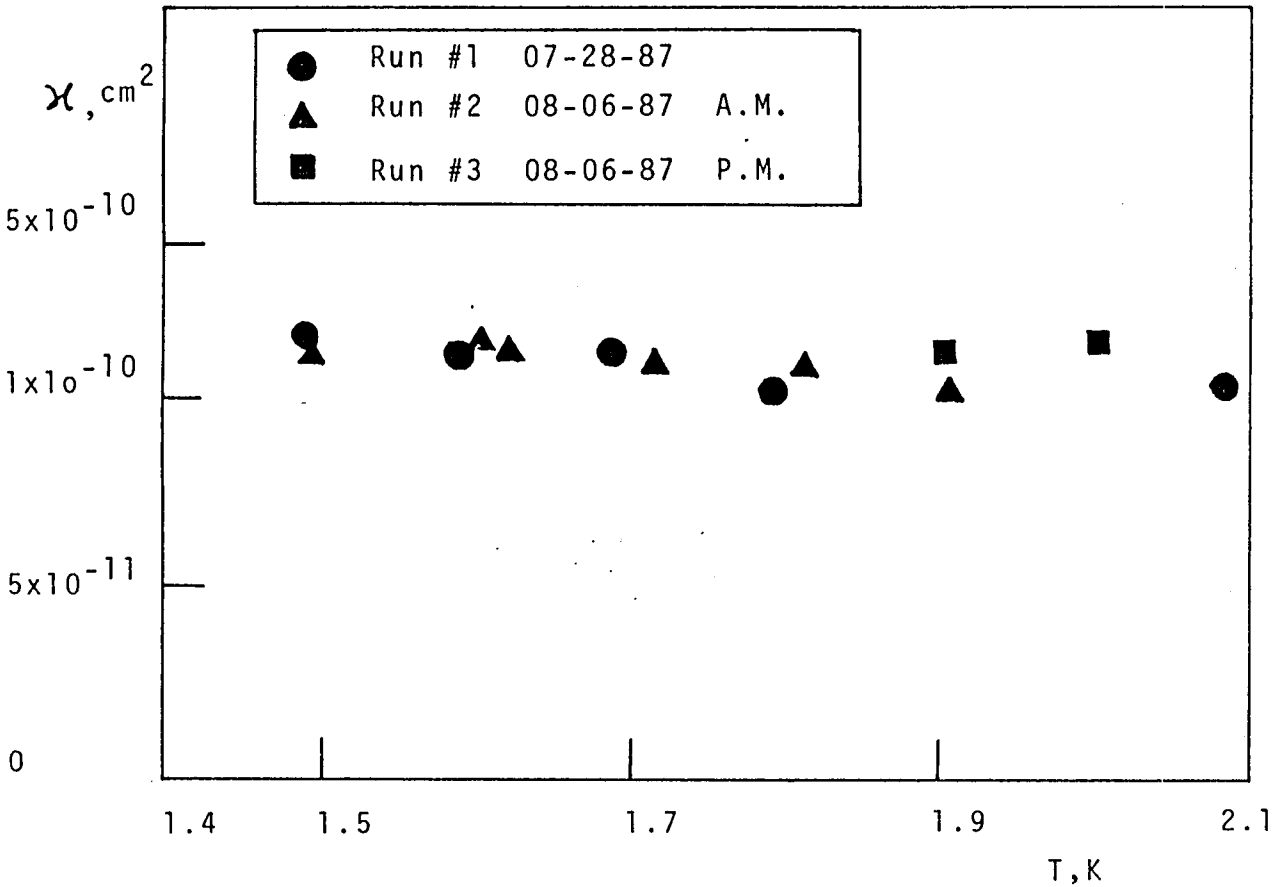

Figure 3.3. Permeability (cm^2) vs Temperature (K).

4. PLUG CHARACTERIZATION: NON-LINEAR REGIME

The rate constants of the non-linear regime of VLPS were evaluated for the first time by Dr. Sidney Yuan in his Ph.D. thesis (UCLA 1985). The constant, designated as K^*_{VLPS}, turned out to be a monotonically increasing function of the permeability. In other words, a size effect on the heat flux density q_o (= superficial value = $\dot{Q}$ divided by the total plug area) is quite distinct. It reduces the flow rates significantly, compared to bulk liquid values. The question has been whether the ZNMF mode would show a similar size effect of the pores, and grains in the plug respectively.

A first survey of the non-linear regime (Appendix B) has shown that similar phenomena apparently prevail in ZNMF systems. However, the small number of data sets is a disturbing factor preventing firm conclusions. Further, slits appear to indicate that the porosity is an important additional parameter of influence. Therefore, the present data sets provide additional evidence. Figure 4.1 is a set of data for the plug K10S02-6.6x0.75. The plug designation and some definitions of factors in the literature are given in Appendix C.

Figure 4.2 presents the data trends of ZNMF rate constants in the non-linear regime based on the usual modified Gorter-Mellink transport function introduced already by S. W. K. Yuan (op. cit.). The rate constant is designated as K^*_{ZNMF}. The ZNMF data indicate indeed a data trend as in VLPS (Figure 4.3). The highest ZNMF rate constant is for a fibrous medium reported previously by the Nijmegen group [1] (compare Appendix B). The second point is from the M.S. thesis of J. M. Lee (UCLA 1983). The lowest rate constant is the preliminary value obtained in the present runs. Though further work is needed, and in progress, it is clear that the rate constants show very similar features in both VLPS and ZNMF modes. In contrast the "pump constants" of FEP operation exhibit very different behavior: they are very weakly dependent on κ for the small permeabilities needed for FEP units. For larger pore sizes, i.e. higher permeabilities, the pump constants appear to tend toward lower values. The

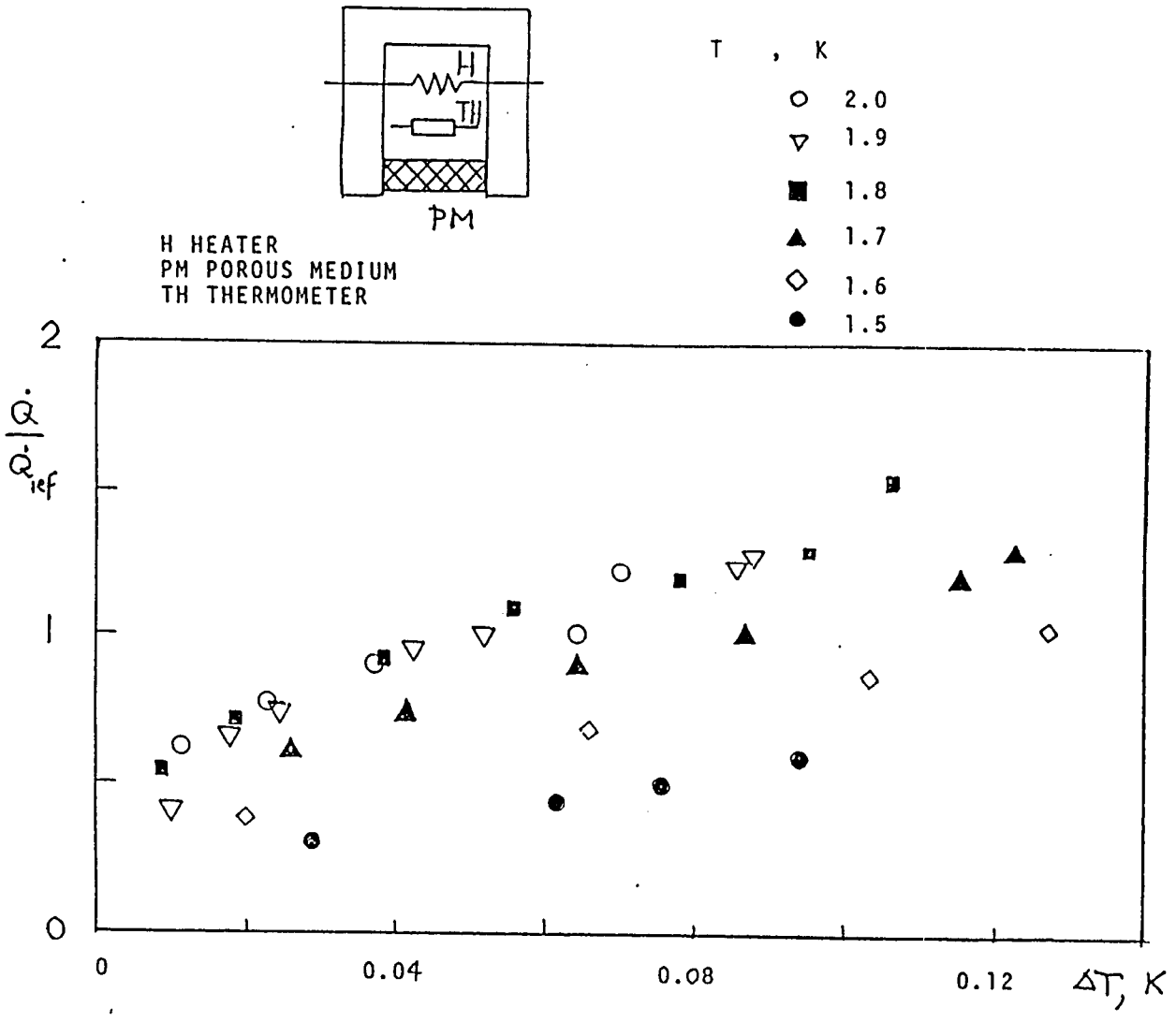

Figure 4.1. Heater power ratio as a function of temperature difference in the non-linear regime.

Inset: ZNMF system for plug measurements.

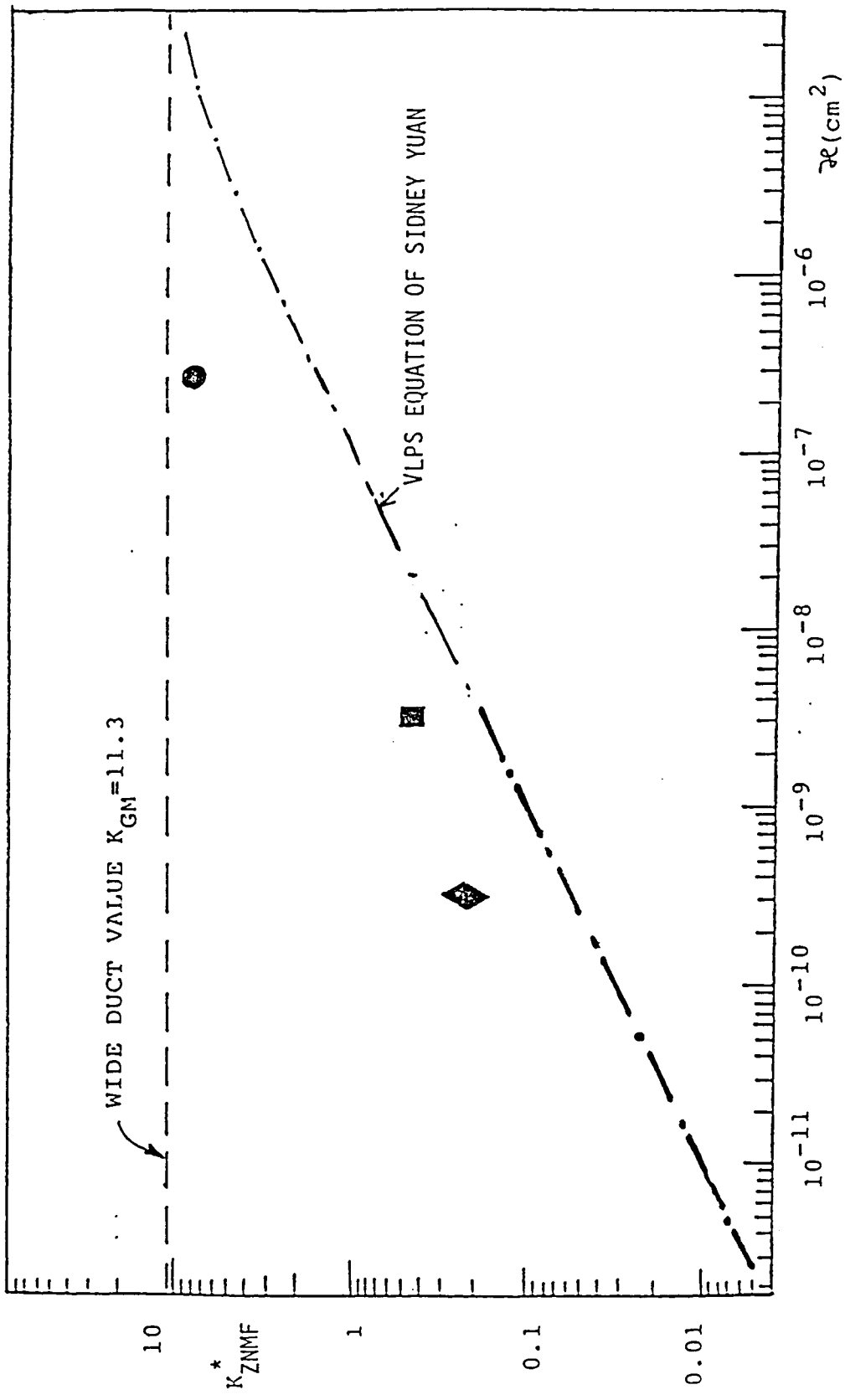

Figure 4.2. Rate constant of ZNMF data sets as a function of permeability. For a comparison the original figure of Dr. Sidney Yuan has been reproduced as Fig. 4.3

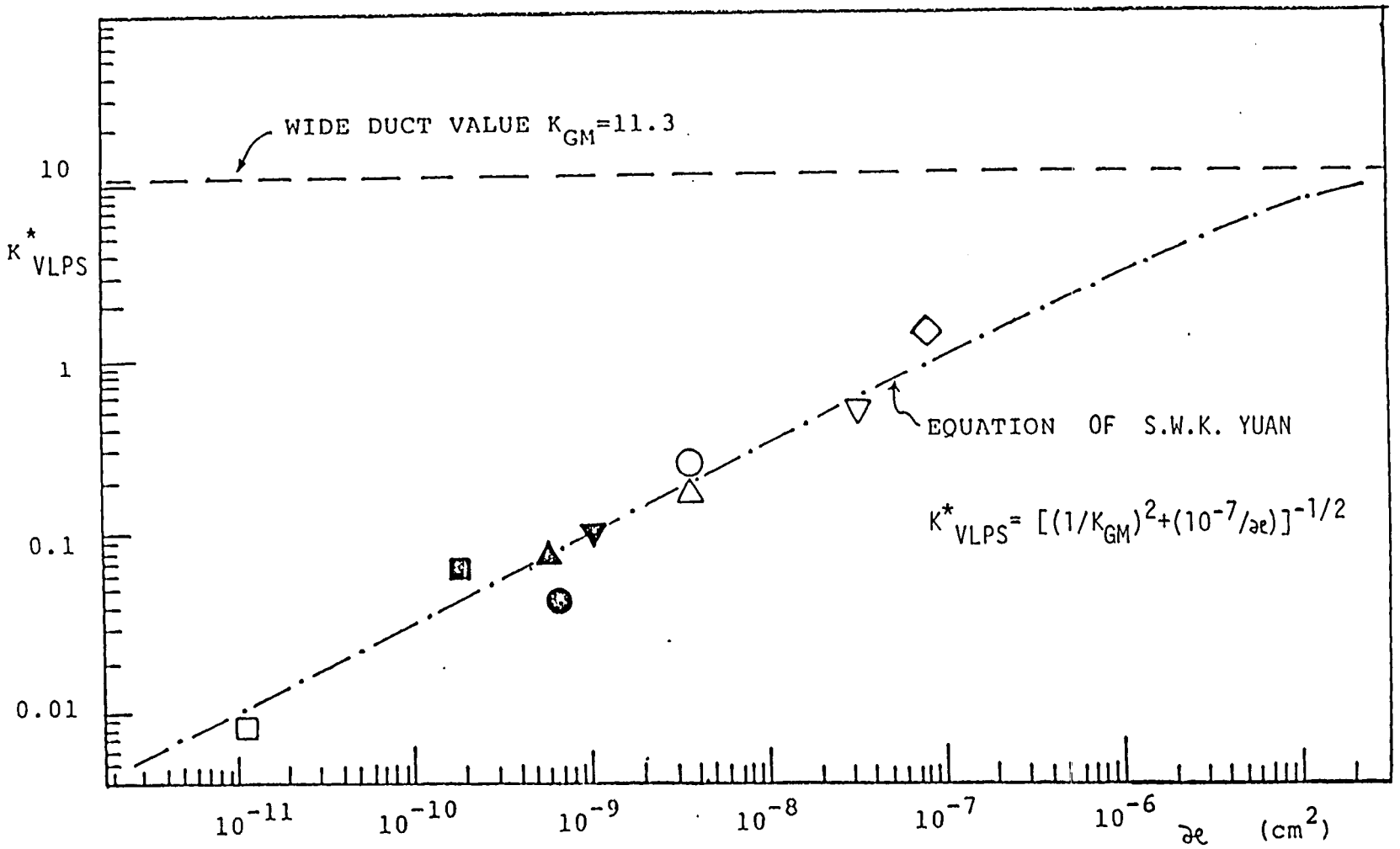

Figure 4.3. VLPS rate constants of Dr. Yuan's thesis.

data do not show a monotonic increase of the "constants" with κ as in VLPS and ZNMF.

5. TEMPERATURE PROFILES IN THE FEP HEATER

This section is a direct continuation of the Summer 1986 work. The FEP unit built has been described by William Chen (op. cit. below). Figure 5.1 is a schematic diagram of the experimental system. The FEP has been aluminum oxide compacted for low permeability. Below this pump core is the heater unit. A U-tube section is located downstream of the heater established as Cu powder plug. The vertical duct after the U-section permits the transition to the FEP flow outlet outside the vacuum can. The liquid is emitted as a jet rising toward the maximum location of the fountain.

The temperature profiles are shown in Figure 5.2 for two bath temperatures. The upper section of the figure is a schematic diagram of the heater system (turned 90 degrees). In principle, the T-profiles may have a domain showing an increase in T along the flow path. However this is seen for low bath temperatures, not at high bath temperatures. The T-increase is in qualitative agreement with data reported by Hofmann et al. (1986) [2] for He II near a pressure of 1 atm. A plausible reason for this T-increase is the monotonic rise of T, for uniform wall heating, using the calorimetric mean temperature. It is noted in addition that the 1 atm pump had a heater wire system wound around the outer tube downstream of the pump plug.

In Figure 5.2 all runs at 1.4 K show a drop in temperature toward the downstream end. This indicates heat leakage toward the downstream liquid. For wide tubes the van Sciver model involves a similar behavior for a certain type of boundary condition. The recent analytical work of Brooks et al. [3] appears to support the van Sciver model for forced flow in wide ducts when wall heating is imposed. However, the present case has different thermal boundary conditions. Further the wide duct equations cannot be applied directly to the present powder of the heater system. Nevertheless certain qualitative features appear to agree with the modified van Sciver theory which is adopted for interpretation.

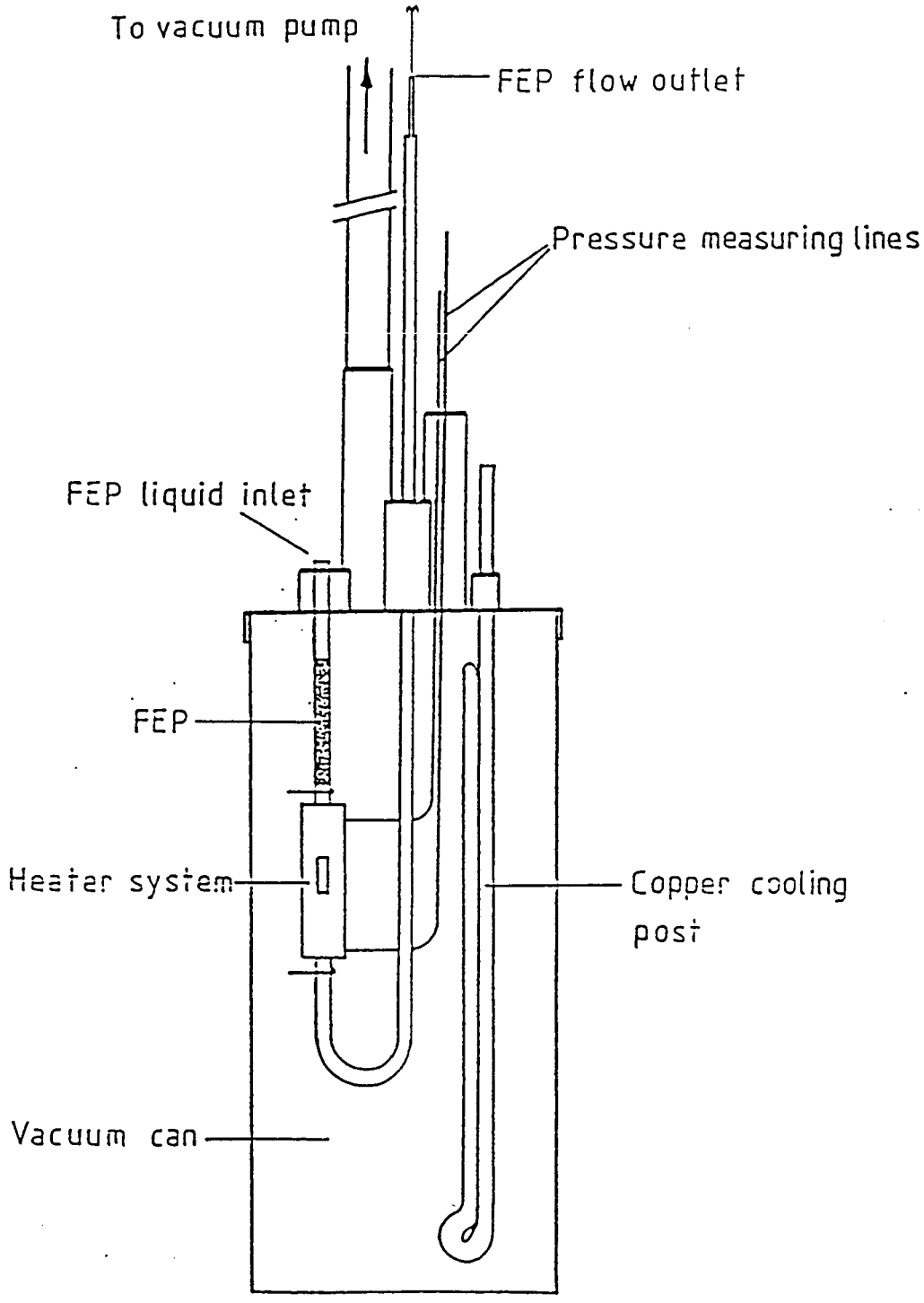

Figure 5.1. Schematic diagram of components arrangement inside vacuum can

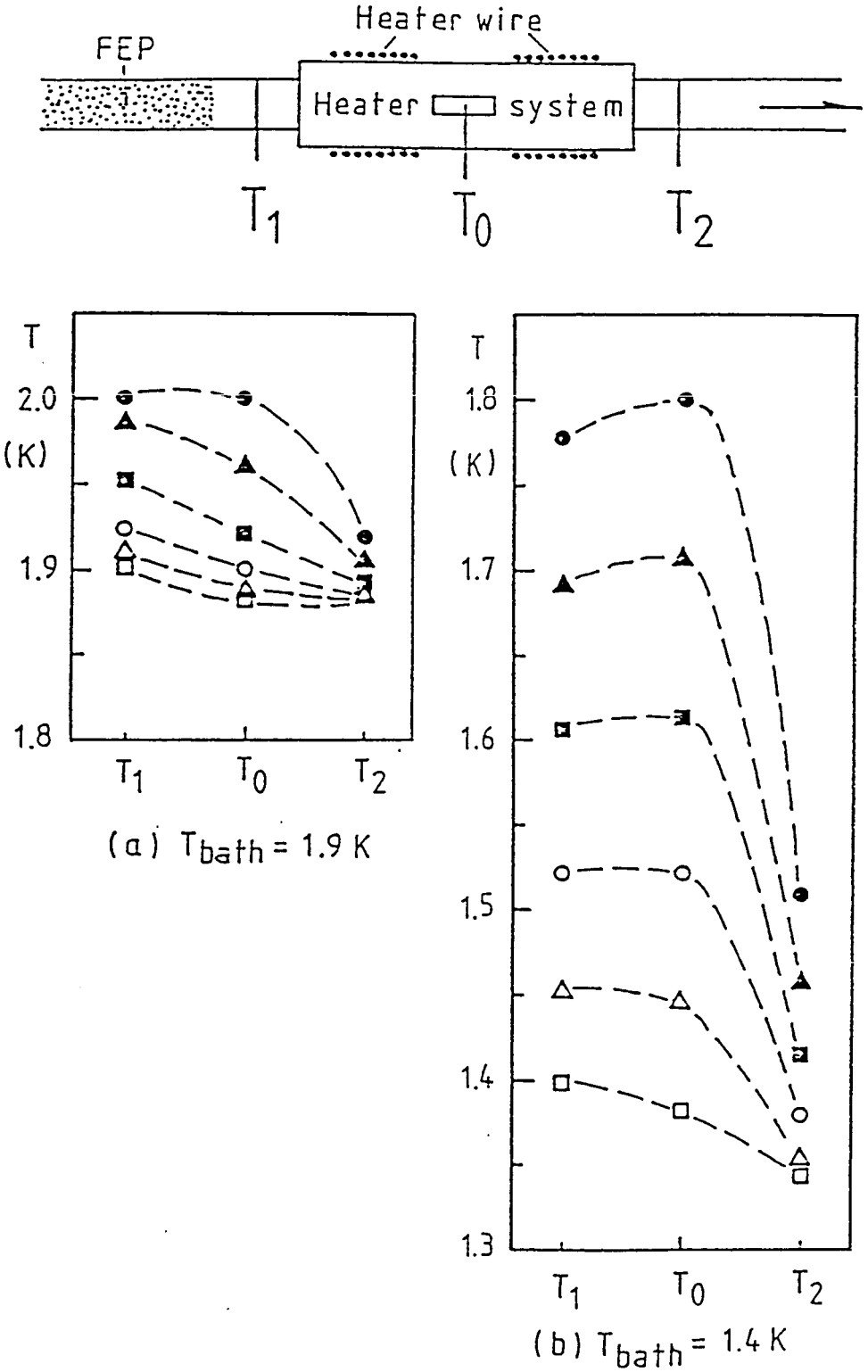

Figure 5.2. The temperature profiles in the direction of liquid flow

A practical concern for efficient FEP units is the heat leakage associated with the T-drop in the heating section. William Chen has proposed (1987)* to prevent excessive leakage using a termination plug of suitable dimensions in order to cut down significantly the outflow rate of thermal energy. The termination plug has the purpose of keeping the heat inside and of raising the energetic effectiveness of the pump as much as possible. The plug at the downstream end has to be of sufficiently small pore size to "leak" little heat. Further it should permit passage of the liquid flow rate. Therefore, it ought to be not too thick.

A particular question relates to the necessity of a termination plug *upstream* of the pump plug. At this location, second law-induced heat flow through solid walls and grains cannot be prevented entirely for fine porous plugs. Further, the liquid in the plug travels in a direction opposite to the second law heat flow. One may object that the ideal superleak (ISL) type models do not permit this type of simplified naive description. However Wilks points out in his book (Wilks 1967) [4] that there is always a departure from an ideal ISL condition, even in very good plugs with near-ideal vortex pinning capability.** Thus, the need for an upstream termination plug, at this stage of our knowledge, appears to be less urgent than the option for a downstream termination plug proposed by William Chen.

*M.Sc. Thesis, UCLA 1987.

**"... Even in the narrowest slits the flow of superfluid will be accompanied by a flow of normal fluid. This will vanish only in the limiting case of an infinitely narrow slit; hence the helium leaving the vessel will never be at absolute zero." [4]

6. ENERGETICS IMPROVEMENTS BASED ON TM FORCE USE

In this section the thermomechanics is inspected first by consideration of historical trends in magnet technology with "hybrid" He II - He I systems, and in space systems. Both developments took place nearly simultaneously, but by and large somewhat independent of each other.

The magnet cooling processes have been initially promoted by the "lambda cooler" arrangement of Roubeau. Roubeau received the Mendelssohn Award for his contributions from the ICEC in 1986 [5]. The system is referred to as "lambda cooler", because very simple means of pumping permit the attainment of the lambda temperature of He II in magnets and other domains to be cooled. A very compact system may result. For large scale magnet applications, such as the "Tore Supra" however, there has to be a stable bath temperature with sufficiently large temperature stability within the He II range. Therefore Claudet, Bon Mardion, Seyfert, Verdier [6] and others were instrumental in modifying the Roubeau type system to get to lower temperatures. Additional system examples are the versions of LBL [7] and Hakuraku et al. [8]. It is noted that a characteristic feature is the use of JT throttling converting He I to He II and using the latent heat of vaporization as a powerful means of lowering the temperature.

The space developments in the low-T area include the IRAS flight system (mentioned above) which is a "passive" system. It is called passive as there is no active refrigerator incorporated. Further, the term "active" is used for VLPS when a controller permits variations of the thermal energy rejection rate while maintaining stable temperatures in the space dewar. A very important feature of space systems may be the lack of a vacuum pump which uses a sizable amount of power for large magnets in terrestrial installations.

The use of TM forces appears to have been proposed explicitly first by Hofmann (1986) [2]. Several items may be distinguished in the area of his proposals. One problem area is the cooling of the superconducting winding package proper. It may be done internally and/or externally using a heat sink. Another problem area is the current lead cooling, the cooling of neck tube sections and other items of this nature. The third item is the refrigerator itself. While all of these points appear to be touched upon in Hofmann's proposed systems, the emphasis has been on a particular experimental setup for which data or calculated results have been obtained (Hofmann et al., 1987) [9]. While interesting R&D work is being performed for magnets near 2 K, there appear to be similar opportunities for space systems with altered specifications, e.g. low mass at launch.

Specific Space-Related TM Force Use. Because of distinctly altered boundary conditions in micro-gravity, the evolution of TM force utilization has different features. A particular point is the initial concentration on VLPS developments mentioned above. The future options of modified TM systems include all of the various subunits which have been discussed so far for various purposes:

vapor-liquid phase separation using the TM force fountain effect transfer pumps (FEP units);

FEP use as "power unit" for vortex refrigeration;

mechano-caloric devices;

cyclic He II vortex refrigerator systems;

heat leak interception devices.

A single TM device may be combined with other components for improvements. The example chosen is heat leak interception. Heat input is used to drive a fountain effect pump (FEP) unit located at the "heat leaking" component. In principle, solar photons and "hot" parts in the space system may supply the heat. In telescope cryovessels filled with He II, the focal plane assembly and related sensor dissipation constitutes a thermal load on the liquid.

Further, support struts have a small, but finite heat input.

Figure 6.1 is a schematic diagram of heat leak interception example along a support rod surrounded by a porous medium which acts as the core of the fountain effect pump (FEP). The incoming heat is diverted to the liquid in a manner which is quite similar to vent tube cooling by escaping vapor in "classical" cryovessels. At the warm end, the He II action is terminated theoretically when the lambda temperature is reached. An alternative, indicated on the left hand side of Figure 6.1, is the routing of the escaping mass into a lambda shield. The experiments of Hofmann et al. [9] indicate that locally He I states may be reached without annihilating He II TM forces. On the right hand side of Figure 6.1 this possibility is indicated. There is a continued He I coolant flow (and subsequently vapor flow) as the escaping mass moves along the rod. On the cold side, the thermal energy to be rejected is the product of temperature times entropy at the low temperature (ST). Thus as the vessel temperature is lowered a smaller and smaller heat rejection is required. Obviously, there is a chance to integrate the heat leak interception with VLPS.

Figure 6.2 is a schematic diagram of a system which uses an interior fluid-filled cylinder for venting. The liquid is to enter a VLPS plug. At the downstream side of this VL^{PS} unit the vapor is removed in the usual way. Installation of these units will produce a lower overall heat input imposed on the vessel's He II. Attractiveness of the various options will depend on the enthalpy difference handled by the system.

The possibility of *refrigeration* by means of heat input has been known as "He II vortex cooler" demonstrated first by Staas and Severijns [10]. The cycle envisioned (Figure 6.3) as the simplest case comprises ideal state changes in ideal superleaks (ISL) and in ideal isobaric heat exchangers (dP = 0). Thus, the sequence is ISL-P-ISL-P, where the first ISL achieves ideal thermomechanical pressure increase, and the second ISL permits mechanocaloric cooling. The cycle has very sharp "corners" in the temperture-entropy diagram (Figure

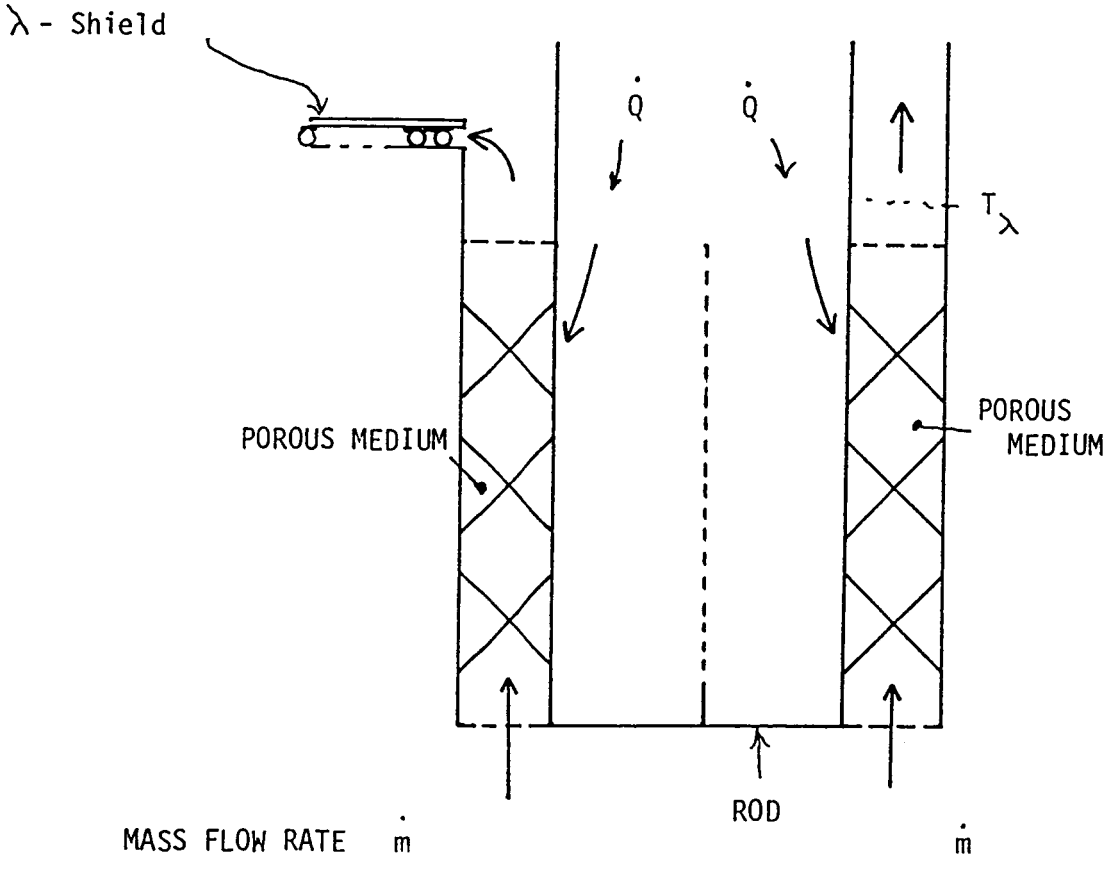

Fig. 6.1. Schematic drawing of liquid cooled solid rod.
a. Option with a "lambda shield";
b. Continued fluid flow along the rod in counterflow to heat flow rate $\dot{Q}$.

Note : Ideal enthalpy difference may not be reached in real system . The entire difference ΔH may decide about system preference for the specs imposed.

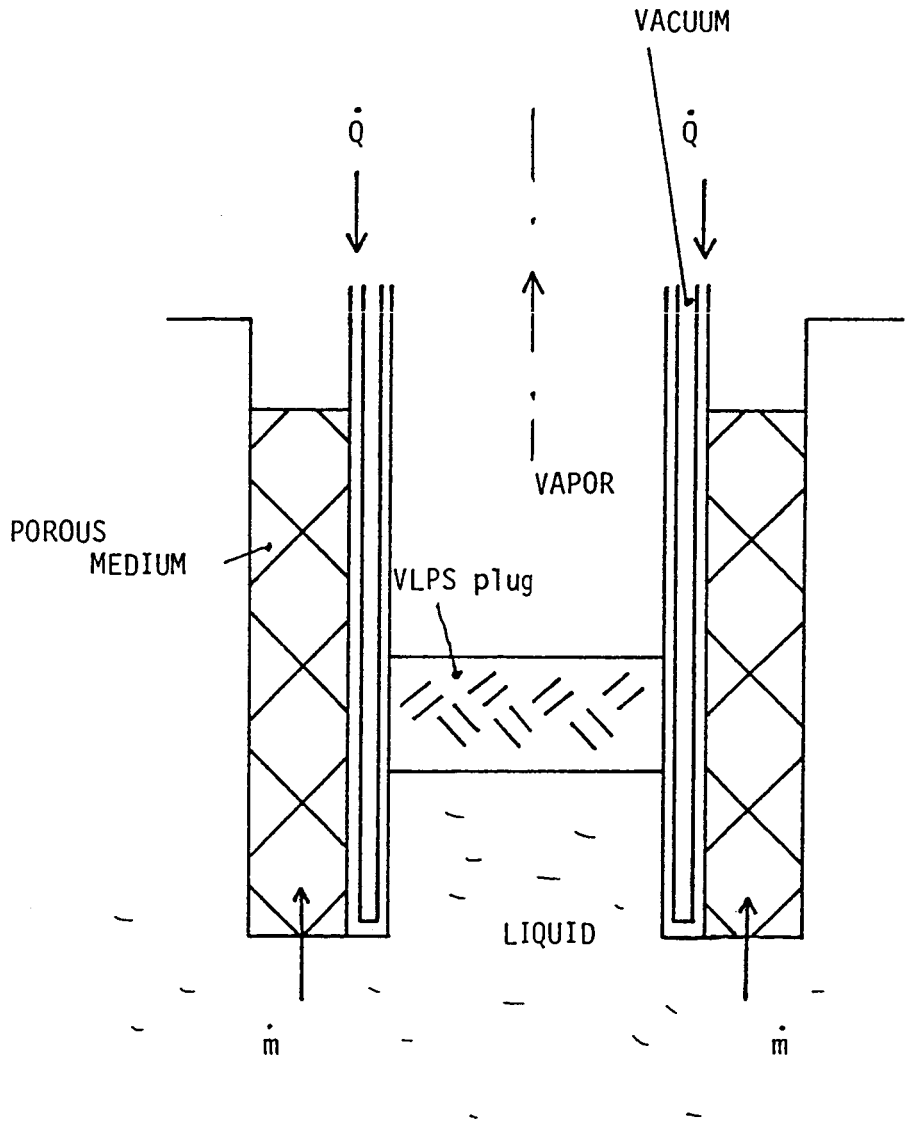

Fig. 6.2. Schematic setup of liquid - cooled tube with interior VLPS plug.
Note : At very low T, the mass flow through the VLPS plug has to be only minute; this option points to the possibility of attaching a "mini vortex fridge" in lieu of the system of Fig. 6.2.

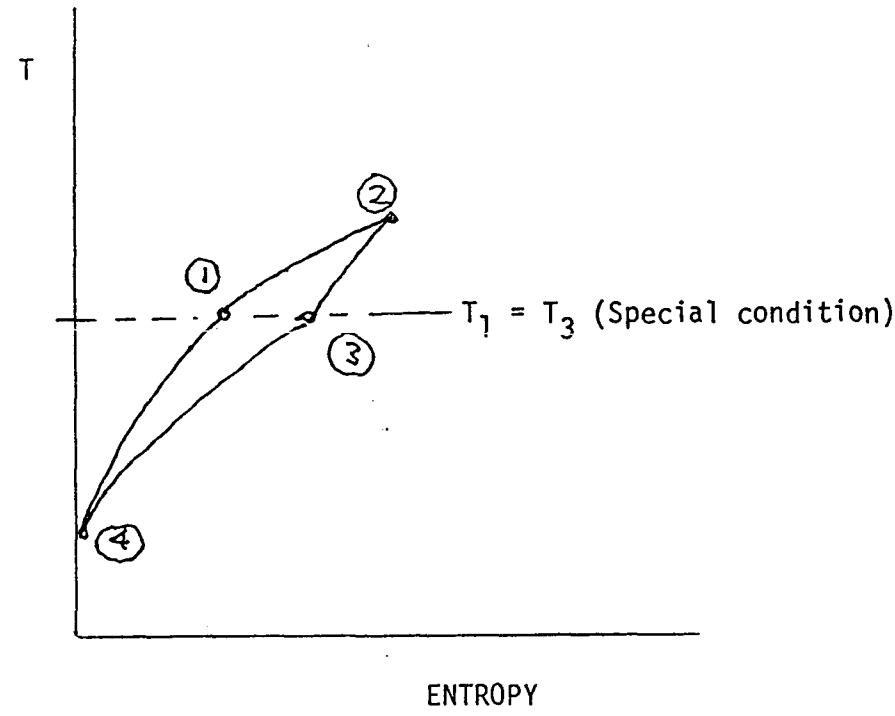

Fig. 6.3 . Simple cycle with ISL pressurization (1-2);
Isobaric aftercooler (2-3);
ISL depressurization (3-4);
Isobaric "cold pickup" (4-1) . NOT TO SCALE!
SCHEMATIC DIAGRAM!

Note : Small area enclosed by this cycle.
The flow power needed for this small area from the thermal energy T_2S_2 appears to be attractive for heat pumping.

6.3) whose enclosed area is very small indicating the attractiveness from the refrigeration point of view. More explicitly, the small area requires only a limited amount of flow power. The sharp changes in dT/dS at the entrance to the first ISL and at the entrance to the second ISL unit point out that great care is needed in het exhanger sizing. In real systems, heat cannot be supplied easily at T-S loctions with zero entropy change. Thus, compact heat exchangers are a necessity for efficient vortex refrigeration.

It is noted that these systems have no moving parts and permit novel device developments for space systems based on the thermomechanical and the mechano-caloric effect. Returning to the question of details of efficient heat leak interception, we note that competing schemes are created (as indicated in Figures 6.2 and 6.2). There appears to be a chance to implement miniaturized vortex refrigeration in order to keep heat out of the vessel while energizing with the external heat input.

We acknowledge the comments of Dr. Sidney Yuan and input of Herbert Simanjuntak.

7. REFERENCES

1. T. H. K. Frederking, H. Van Kempen, M. A. Weenen and P. Wyder, Physica 108B, 1129, 1981.
2. A. Hofmann et al., ICEC-11 Berlin, Butterworth, 1986, p. 312.
3. J. H. Lee, Y. S. Ng and W. F . Brooks, 1987 Space Cryog. Workshop, Madison, WI, paper A-5; also paper AIAA-87-1495, 1987.
4. J. Wilks, Liquid and Solid Helium, Oxford, Clarendon, 1967, p. 43.
5. Proceedings ICEC-11, Butterworths, 1986.
6. G. Bon Mardion, G. Claudet et al., Adv. Cryog. Eng. 23, 1978, p. 362.
7. R. P. Warren et al., Proc. ICEC-8, 1980, p. 373.
8. Y. Hakuraku and H. Ogata, Cryogenics 23, 1983, p. 291.
9. A. Hofmann et al., Cryog. Eng. Conf., 1987, paper BC-5.
10. F. A. Staas and A. P. Severijns, Cryogenics 9, 1969, p. 422.

POROUS PLUG IDENTIFICATION AND THROUGHPUT PARAMETERS

The initial years of porous plug work focused on vapor-liquid phase separation with rather large physical dimensions of sintered plugs. For instance 1 in. diameter (2.54 cm) plugs and 1/2 in. O.D. plugs have been used. An example is given in Figure C.1. The first item is the source of the plug (manufacturer, distributor). The second number is the nominal filtration rating, i.e. the particle size retained during filtration usually involving fluid-solid separation. The third item is the material, e.g. s = stainless steel. The fourth number is the identification number for the particular plug of the type specified by the first three pieces of information. The fifth number is the diameter of the plug. The sixth figure is the thickness.

Our recent emphasis of other plug applications has introduced smaller permeabilities. Therefore, a different classification scheme has been used called category II (Figure C.2). The dimensions at the end of the identification sequence are given in mm. An example is PK 10 S 02 - 6.4 x 7.5. The diameter of this example of category II is 6.4 mm, and the thickness is 0.75 mm.

The throughput capability measure, preferred in our work is th Darcy permeability (κ) or its reciprocal value ($1/\kappa$) which is a d.c. resistance measure. However, other quantities are used in the literature. An example is the "F" factor of Petrac (Low Temp. Phys. LT 14, ed. M. Krusius, M. Vuorio, North Holland, Vol. 4, 1975, p. 33).

$$\dot{Q} = \dot{W}_r = F\ A\ \Delta P \tag{C.1}$$

$\dot{W}_r$ = refrigeration capacity (= heat flow rate), A area, ΔP pressure difference. The heat transported is formulated as the product of the normal fluid velocity times the porosity, A and $\rho\overline{ST}$, where $\rho\overline{ST}$ is the mean entropy per unit volume.

CATEGORY I

EXAMPLE

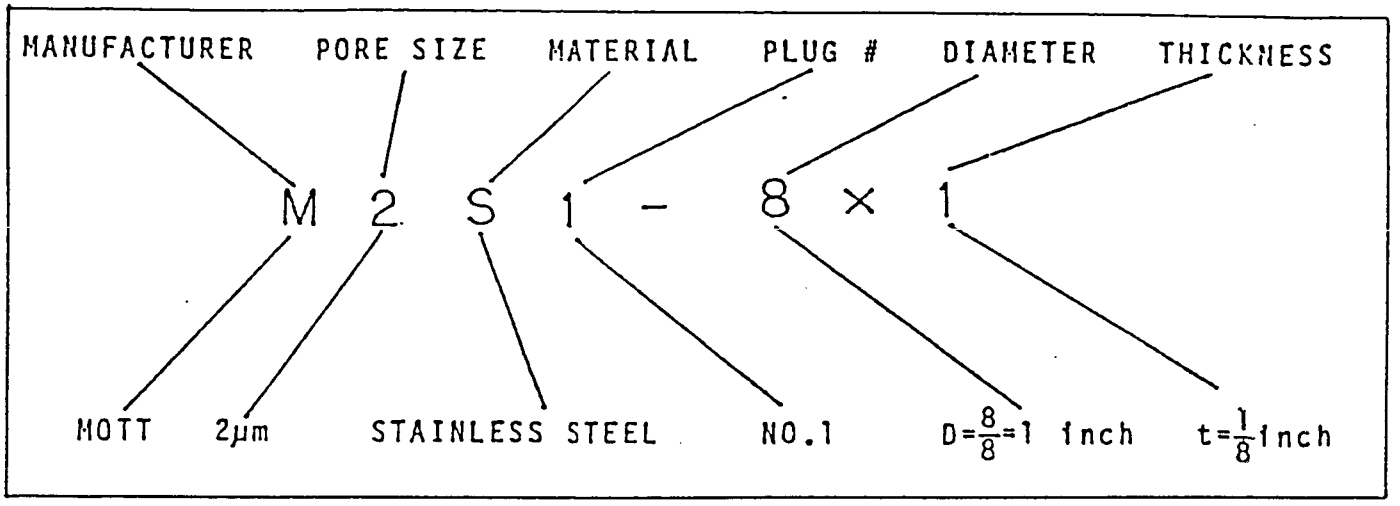

Fig. C.1. Porous plug identification system

CATEGORY II

EXAMPLE

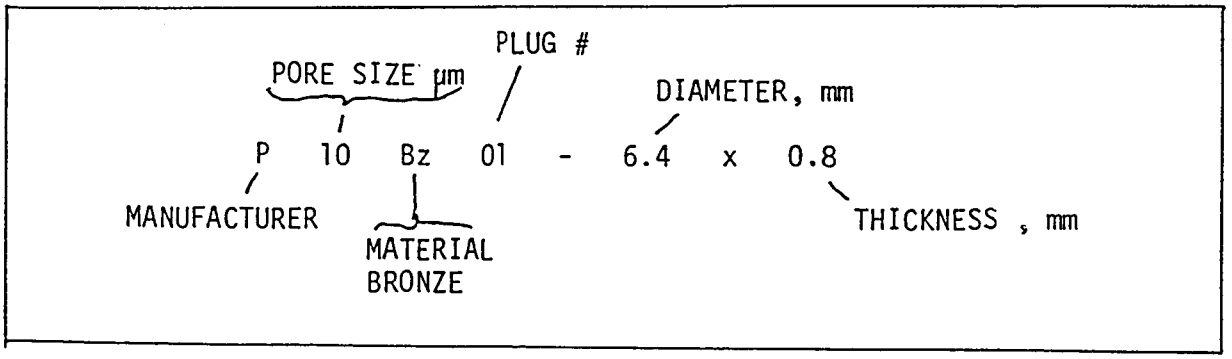

Fig. C.2. Porous plug identification system for present small-pore plugs with small outer dimensions

Another example is the heat exchanger-related flow quantity definition of Wheatley et al. (Rev. Sci. Instru. 41, 147, 1971). The factor is denoted as "Z" (= d.c. flow impedance factor).

$$Z = \Delta P/(\dot{V}\eta) \tag{C.2}$$

η = shear viscosity, $\dot{V}$ volumetric flow rate. The Z factor is related to the Darcy permeability by

$$Z = \kappa^{-1}L/A \tag{C.3}$$

L thickness of plug (or length of flow path). An example in the area of porous media has been given by Ahlers and Singsaas (Phys. Rev. B19, 1984, 4951). The powder system of these authors is for the establishment of fountain pressure differences. The κ-values are on the order of 10^{-11} cm^2.

APP. D

THERMOMETER CALIBRATION AT VERY SMALL TEMPERATURE DIFFERENCES

The carbon resistor thermometers used are Allen - Bradley, 39 Ohm, resistors. The calibration procedure involves the measuring of the thermometer's resistance and the corresponding vapor pressure of the system. The properties of the thermometer are such that the resistance is approximately logarithmically proportional to the vapor pressure. This can be expressed as:

$$\ln (R) = a \ln (Pv) + b \qquad (D.1)$$

R = Thermometer resistance
Pv = Vapor pressure
a,b = Linear least square parameters

Therefore, by using a temperature-vapor pressure curve, such as the T-58 scale, the temperature versus resistance relationship is derived for small temperature difference. A printout of a sample computer program and its output shows the utilization of a T-58 cubic spline fit (fit presented by Donnelly, R.J., et al in *J. Low Temp. Phys., 1981)* for iterative resistance-temperature calculations (Tables D1 and D2).

For very small T-differences, the calibration equation (D.1) permits a convenient determination of ΔT from the resistance difference ΔR. The slope of the vapor pressure curve is known from the T-58 scale:

$$\Gamma = P_v^{-1} \, dP_v/dT \qquad (D.2)$$

Inserting d ln R/d ln Pv = a = $(dR/R)/(dP_v/Pv)$ one obtains

$$\Delta T = \Delta R \, dT/dR = \Delta R \, (aR\Gamma)^{-1} \qquad (D.3)$$
$$\Delta T << T$$
$$R = R_0$$

$R = R_0$ at the bath temperature.

Table D1. Program sample

```
10 DIM A(25), Q(29), D(4), F(4), S(4)
20 B=8.8442:AL=-.4921
25 GOSUB 1000
27 GOSUB 3000
28 END
180 IF P < 120.007 OR  P > 7600001  THEN RETURN
185 P = LOG (P)/2.303
190 T1=1
200 T2=4.215
210 X=(T1+T2)/2
220 GOSUB 340
230 IF ABS(D(1)-P) < .000001 THEN 290
225 REM
240 IF D(1)>P THEN 270
250 T1=X
260 GOTO 210
270 T2=X
280 GOTO 210
290 D(1) = 10^D(1)
300 F(1)=D(1)*F(1)
310 S(1)=D(1)*(S(1)+(F(1)/D(1))^2)
320 TE=X
330 RETURN
340 I=0
350 J=22
360 K=(I+J)/2
370 IF J-I<= 1 THEN 430
380 IF X>Q(K+4) THEN 410
390 J=K
400 GOTO 360
410 I=K
420 GOTO 360
430 FOR I = 1 TO 4
440 S(I)=0
450 F(I)=0
460 D(I)=A(I+J-1)
470 NEXT I
480 FOR K = 1 TO 3
490 FOR I = 1 TO 4-K
500 P1=X-Q(I+J+K-1)
510 P2=Q(I+J+3)-X
520 P3=1/(Q(I+J+3)-Q(I+J+K-1))
530 S(I)=(P1*S(I+1)+P2*S(I)+2*(F(I+1)-F(I)))*P3
540 F(I)=(P1*F(I+1)+P2*F(I)+D(I+1)-D(I))*P3
550 D(I)=(P1*D(I+1)+P2*D(I))*P3
560 NEXT I
570 NEXT K
580 RETURN
1000 FOR I = 1 TO 29
1010 READ Q(I)
1020 NEXT I
1030 FOR I = 1 TO 25
1040 READ A(I)
1050 NEXT I
1060 RETURN
2000 DATA 1,1,1,1
2010 DATA 1.15105499, 1.28765750, 1.43202085, 1.59832713
2020 DATA 1.74054952, 1.89959361, 2.10178990, 2.17601406, 2.16321995
2030 DATA 2.28846654, 2.57937753, 2.74048335, 2.88959932, 3.04057357
2040 DATA 3.18965645, 3.34056636, 3.47966198, 3.63056679, 3.77966011
2050 DATA 3.92027624, 4.0700000
2060 DATA 4.125, 4.125, 4.125, 4.125
2070 DATA 2.07920530, 2.29041820, 2.64118049, 3.06764295
2080 DATA 3.43487191, 3.74460242, 4.01673570, 4.26906294, 4.45301104
2090 DATA 4.55807916, 4.62414591, 4.76041382, 4.92371929, 5.07893104
2100 DATA 5.18829011, 5.28706835, 5.27948565, 5.46374572, 5.54338324
2110 DATA 5.61826745, 5.68927627, 5.75653645, 5.82003175, 5.86106883
2120 DATA 5.88031258
3000 LPRINT "RESISTANCE","TEMPERATURE"
3005 LPRINT "   (OHMS)","   (DEG K)"
3010 FOR X = 1 TO 3.4 STEP .01
3020 GOSUB 340
3030 P = 10^D(1)/1000
3040 R = EXP(AL*LOG(P)+B)
3050 LPRINT R,INT(X*100+.5)/100
3060 NEXT X
3070 RETURN
```

Table D2. Program Output Sample

RESISTANCE (OHMS)	TEMPERATURE (DEG K)
19683.85	1
18777.66	1.01
17927.31	1.02
17128.68	1.03
16377.96	1.04
15671.68	1.05
15006.67	1.06
14380	1.07
13788.96	1.08
13231.06	1.09
12704.02	1.1
12205.72	1.11
11734.24	1.12
11287.75	1.13
10864.6	1.14
10463.24	1.15
10082.28	1.16
9720.429	1.17
9376.506	1.18
9049.441	1.19
8738.213	1.2
8441.889	1.21
8159.563	1.22
7890.427	1.23
7633.71	1.24
7388.695	1.25
7154.698	1.26
6931.108	1.27
6717.332	1.28
6512.823	1.29
6317.063	1.3
6129.609	1.31
5950.002	1.32
5777.861	1.33
5612.778	1.34
5454.409	1.35
5302.397	1.36
5156.438	1.37
5016.218	1.38
4881.452	1.39
4751.878	1.4
4627.239	1.41
4507.283	1.42
4391.802	1.43
4280.565	1.44
4173.385	1.45
4070.073	1.46
3970.46	1.47
3874.389	1.48
3781.687	1.49
3692.216	1.5
3605.832	1.51
3522.4	1.52
3441.795	1.53
3363.892	1.54
3288.579	1.55
3215.747	1.56
3145.289	1.57
3077.1	1.58
3011.095	1.59

RESISTANCE (OHMS)	TEMPERATURE (DEG K)
2947.177	1.6
2885.263	1.61
2825.275	1.62
2767.135	1.63
2710.777	1.64
2656.13	1.65
2603.128	1.66
2551.708	1.67
2501.817	1.68
2453.39	1.69
2406.374	1.7
2360.722	1.71
2316.375	1.72
2273.293	1.73
2231.424	1.74
2190.727	1.75
2151.162	1.76
2112.686	1.77
2075.263	1.78
2038.858	1.79
2003.437	1.8
1968.964	1.81
1935.409	1.82
1902.741	1.83
1870.93	1.84
1839.946	1.85
1809.763	1.86
1780.352	1.87
1751.692	1.88
1723.756	1.89
1696.52	1.9
1669.962	1.91
1644.063	1.92
1618.802	1.93
1594.161	1.94
1570.12	1.95
1546.663	1.96
1523.773	1.97
1501.434	1.98
1479.628	1.99
1458.344	2
1437.564	2.01
1417.275	2.02
1397.462	2.03
1378.11	2.04
1359.212	2.05
1340.748	2.06
1322.712	2.07
1305.089	2.08
1287.368	2.09
1271.039	2.1
1254.589	2.11
1238.514	2.12
1222.803	2.13
1207.45	2.14
1192.449	2.15
1177.792	2.16
1163.472	2.17
1149.487	2.18
1135.801	2.19